Supplementary Figures

Supplemental Figure 1. Immune cell composition is not altered in the absence of HECTD3. (**A**) Targeting strategy used to generate *Hectd3*$^{-/-}$ mice and primers used for genotyping. (**B**) Genotyping of offspring generated from breeding of *Hectd3* heterozygous mice. (**C**) Western blot analysis of HECTD3 in the liver, kidney, and brain of WT and *Hectd3*$^{-/-}$ mice. (**D**) Flow cytometry analysis of $CD4^+$ T cells, $CD8^+$ T cells, B cells, and neutrophils in the bone marrow (BM), spleen, and peripheral blood from WT and *Hectd3*$^{-/-}$ mice. (**E**) Flow cytometry analysis of dendritic cells in the spleen from WT and *Hectd3*$^{-/-}$ mice. (**F**) Flow cytometry analysis of macrophages in the spleen from WT and *Hectd3*$^{-/-}$ mice. (**G**) Flow cytometry analysis of basophils in BM from WT and *Hectd3*$^{-/-}$ mice. Data represent 3 independent experiments.

Supplemental Figure 2. HECTD3 deficiency attenuates the susceptibility of mice to *F. novicida* infection. (**A**) *Hectd3*$^{-/-}$ mice and littermate WT controls were infected subcutaneously with *F. novicida* (3.0×10^5 CFUs) for 2 days. WT mice exhibited ruffled fur and hunched back. (**B**) Production of TNF-α, IL-6, IL-1β, and IFN-β in sera from WT and *Hectd3*$^{-/-}$ mice infected with *F. novicida* for 2 days. Data represent 3 independent experiments and are presented as mean±SEM. *, $P<0.05$; ***, $P<0.001$; ns, not significant.

Supplemental Figure 3. Immune cell composition in lungs is comparable between WT and *Hectd3*$^{-/-}$ mice at 12 h after intranasal infection with *F.*

***novicida*.** (**A**-**C**) *Hectd3*$^{-/-}$ mice and littermate WT controls were intranasally infected with *F. novicida* (800 CFUs per mouse) for 3 days, and bacterial burden was analyzed in the lungs (**A**), peripheral blood (**B**), and spleen (**C**). (**D**–**G**) *Hectd3*$^{-/-}$ mice and littermate WT controls were intranasally infected with GFP-expressing *F. novicida* (5,000 CFUs per mouse) for 12 h. (**D**) Bacterial burden was analyzed in lungs of WT and *Hectd3*$^{-/-}$ mice after *F. novicida* infection. (**E**) Flow cytometry analysis of total macrophages and GFP^{+} macrophages in lungs of WT and *Hectd3*$^{-/-}$ mice after *F. novicida* infection. (**F**) Flow cytometry analysis of total neutrophils and GFP^{+} neutrophils in lungs of WT and *Hectd3*$^{-/-}$ mice after *F. novicida* infection. (**G**) Flow cytometry analysis of total B cells and T cells in lungs of WT mice after *F. novicida* infection. Each symbol indicates an individual mouse. Data represent 2 independent experiments and are presented as mean±SEM. *, $P<0.05$; **, $P<0.01$; ns, not significant.

Supplemental Figure 4. Differentially expressed genes in uninfected and *F. novicida*–infected WT and *Hectd3*$^{-/-}$ BMDMs. (**A**) RNA sequencing analysis of gene expression in uninfected and *F. novicida*–infected WT and *Hectd3*$^{-/-}$ BMDMs for 8 (*F. n* 8 h) and 12 (*F. n* 12 h) h, respectively. Differentially expressed genes in WT and *Hectd3*$^{-/-}$ BMDMs are shown. (**B**) Differentially expressed genes in *F. novicida*–infected WT BMDMs for 8 h (WT_8) versus uninfected WT BMDMs (WT_0). (**C**) Differentially expressed genes in *F. novicida*–infected *Hectd3*$^{-/-}$ BMDMs for 8 h (KO_8) versus uninfected *Hectd3*$^{-/-}$ BMDMs (KO_0). (**D**) Differentially expressed genes in *F. novicida*–infected WT

BMDMs for 12 h (WT_12) versus uninfected WT BMDMs (WT_0). (**E**) Differentially expressed genes in *F. novicida*–infected *Hectd3*$^{-/-}$ BMDMs for 12 h (KO_12) versus uninfected *Hectd3*$^{-/-}$ BMDMs (KO_0). Red and green dots indicate upregulated and downregulated genes, respectively.

Supplemental Figure 5. HECTD3 mediates type I IFN production in response to *F. novicida*, *Mycobacterium*, *Listeria*, and *E. coli* infection. (**A**) BMDMs from WT and *Hectd3*$^{-/-}$ mice were infected with *F. novicida* (100 MOI) for indicated times, and expression of *Ifit*, *Irf1*, *Isg15*, *Il6*, *Il1a*, and *Hectd3* was analyzed by qRT-PCR. (**B**) BMDMs from WT and *Hectd3*$^{-/-}$ mice were infected with BCG-GFP (100 MOI) for indicated times, and expression of *Ifnb*, *Cxcl9*, *Irf1*, *Mx1*, *Ifng*, *Il6*, *Tnfa*, and *Hectd3* was analyzed by qRT-PCR. (**C**) BMDMs from WT and *Hectd3*$^{-/-}$ mice were infected with *L. monocytogenes* (20 MOI) for indicated times, and gene expression of *Ifnb*, *Cxcl9*, *Irf1*, *Mx1*, *Il6*, and *Tnfa* was analyzed by qRT-PCR. (**D**) BMDMs from WT and *Hectd3*$^{-/-}$ mice were infected with *E. coli* (100 MOI) for indicated times, and expression of *Ifnb*, *Cxcl9*, *Irf1*, *Mx1*, *Il6*, and *Tnfa* was analyzed by qRT-PCR. Data represent 3 independent experiments and are presented as mean±SEM. *, $P<0.05$; **, $P<0.01$; ***, $P<0.001$; ****, $P<0.0001$; ns, not significant.

Supplemental Figure 6. HECTD3 mediates type I IFN production in response to HSV infection. (**A**) BMDMs from WT and *Hectd3*$^{-/-}$ mice were infected with HSV (3 MOI) for indicated times, and expression of *Ifnb*, *Cxcl9*, *Mx1*,

Irf1, *Tnf*, and *Hectd3* was analyzed by qRT-PCR. (**B**) Immunoblot analysis of phosphorylation of TBK1 and IRF3, and total TBK1 and IRF3 in uninfected and HSV–infected WT and *Hectd3*$^{-/-}$ BMDMs. Data represent 2 independent experiments and are presented as mean±SEM. *, P<0.05; **, P<0.01; ***, P<0.001; ns, not significant.

Supplemental Figure 7. Cell death is reduced in *Hectd3*$^{-/-}$ BMDMs during *F. novicida* infection. (**A**) Immunoblot analysis of caspases 1, 3, 8 and 11, ZBP1, and MLKL phosphorylation in uninfected and *F. novicida*–infected WT and *Hectd3*$^{-/-}$ BMDMs for 14 h. GAPDH was used as loading control. (**B**) LDH release in uninfected and *F. novicida*-infected WT and *Hectd3*$^{-/-}$ BMDMs for 14 h. (**C**) Microscopy analysis of uninfected and *F. novicida*–infected WT and *Hectd3*$^{-/-}$ BMDMs for 14 h. Data represent 3 independent experiments. Scale bars, 20 μm for (**C**).

Supplemental Figure 8. HECTD3 is required for inflammasome activation during *Mycobacterium* and *Listeria* infection. (**A**) WT and *Hectd3*$^{-/-}$ BMDMs were stimulated with lipopolysaccharide and ATP for NLRP3 inflammasome activation and infected with *Salmonella* for NLRC4 inflammasome activation. (**B** and **C**) WT and *Hectd3*$^{-/-}$ BMDMs were transfected with plasmid DNA (**B**) or poly(dA:dT) (**C**) for canonical AIM2 inflammasome activation. (**D**) Immunoblot analysis of LC3, TFEB, and HECTD3 in uninfected BMDMs and WT and *Hectd3*$^{-/-}$ BMDMs infected with *F. novicida* for indicated times. (**E**) Inflammsome

activation was detected in WT and *Hectd3*$^{-/-}$ BMDMs infected with BCG-GFP or *Listeria*. Supernatant (Sup) was used to detect cleaved caspase 1; cell lysate (Cell) was used for pre-caspase-1, HECTD3, and GAPDH blotting. GAPDH was used as loading control. Data represent 3 independent experiments.

Supplemental Figure 9. HECTD3 is essential for TRIF- and STING-dependent type I IFN production. (**A**) Gene expression analysis of WT and *Hectd3*$^{-/-}$ BMDMs in response to Pam3CSK4 stimulation for indicated times. (**B**) Gene expression analysis of WT and *Hectd3*$^{-/-}$ BMDMs in response to imiquimod or CpG ODN stimulation for indicated times. (**C**) Gene expression analysis of WT and *Hectd3*$^{-/-}$ BMDMs in response to poly(I:C) or dsRNA transfection treatment for indicated times. (**D**) Gene expression analysis of WT and *Hectd3*$^{-/-}$ MEFs in response to poly(I:C) or dsRNA transfection treatment for indicated times. Data represent 3 independent experiments and are presented as mean±SEM. *, $P<0.05$; ns, not significant.

Supplemental Figure 10. HECTD3 interacts with TRIF, STING and TBK1. Immunoblot analysis of HECTD3 that co-immunoprecipitated with FLAG-tagged TRIF, STING, and TBK1 from lysates of HEK293T cells transfected with plasmids as indicated. Data represent 3 independent experiments.

Supplemental Figure 11. HECTD3-mediated TRAF3 polyubiquitination and TBK1 activation. (**A**) Co-IP analysis of K6-, K11-, K27-, K29-, K33- or K0 (all

Lysine residues were mutated)-linked polyubiquitination of TRAF3 mediated by HECTD3 in HEK293T cells transfected with plasmids as indicated. K48+MG132 indicates detection of K48-linked polyubiquitination of TRAF3 in the presence of MG132 treatment. (**B**) Upon bacterial infection, TLR4, TLR3, and cGAS engagements recruit adaptor proteins TRIF and STING to activate TRAF3. In turn, HECTD3-mediated K63-linked polyubiquitination of TRAF3 facilitates the activation of TBK1 by TRAF3-associated complexes and type I IFN induction. Data represent 2 independent experiments for (**A**).

Supplementary Tables

Supplemental Table 1. Upregulated genes. Comparison of genes upregulated in uninfected WT BMDMs versus uninfected *Hectd3*$^{-/-}$ BMDMs; WT BMDMs infected with *F. novicida* for 8 h versus *Hectd3*$^{-/-}$ BMDMs infected with *F. novicida* for 8 h; WT BMDMs infected with *F. novicida* for 12 h versus *Hectd3*$^{-/-}$ BMDMs infected with *F. novicida* for 12 h; WT BMDMs infected with *F. novicida* for 8 h versus uninfected WT BMDMs; *Hectd3*$^{-/-}$ BMDMs infected with *F. novicida* for 8 h versus uninfected *Hectd3*$^{-/-}$ BMDMs; WT BMDMs infected with *F. novicida* for 12 h versus uninfected WT BMDMs; and *Hectd3*$^{-/-}$ BMDMs infected with *F. novicida* for 12 h versus uninfected *Hectd3*$^{-/-}$ BMDMs.

Supplemental Table 2. Primer sequences for real-time qPCR.

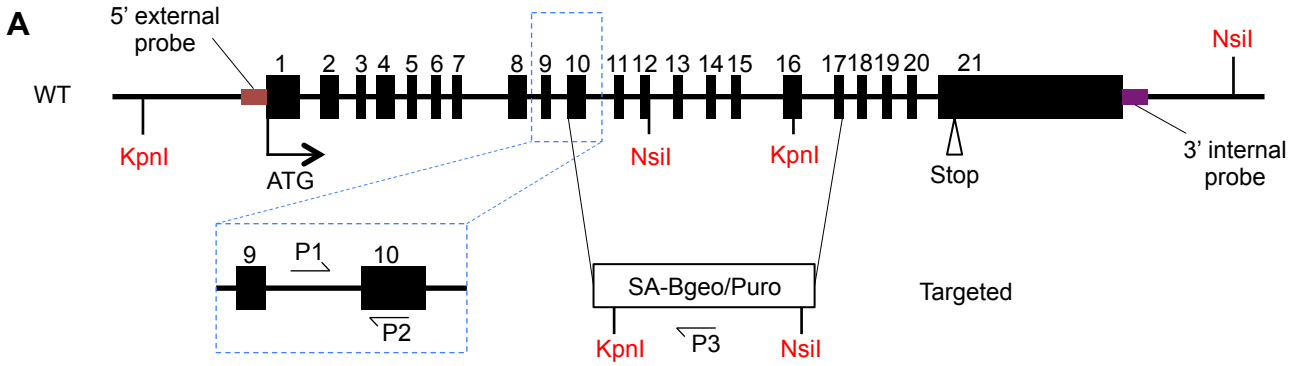

B

Genotyping Strategies

Primer pairs	P1 and P2	P1 and P3
WT	210 bp	No
Hectd3$^{-/-}$	No	427 bp
Hectd3$^{+/-}$	210 bp	427 bp

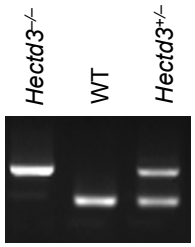

C

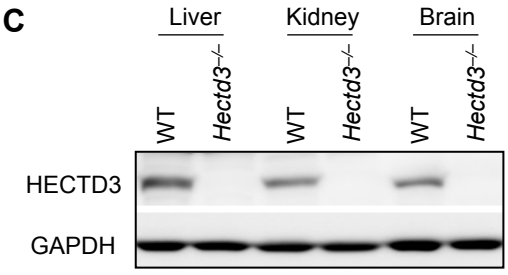

D

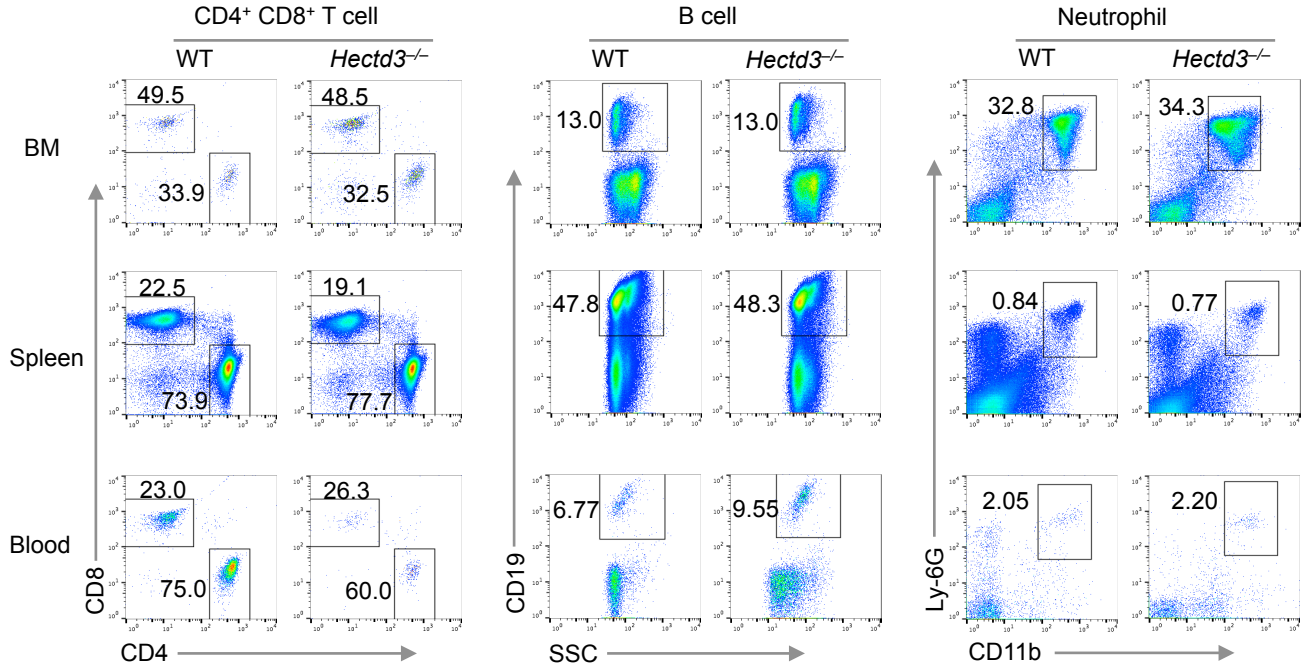

E

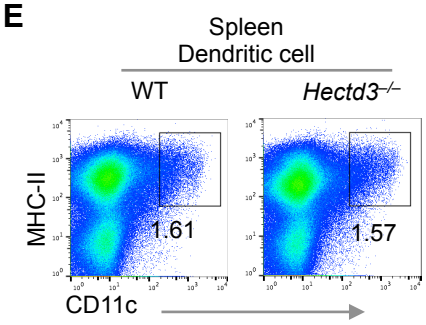

F

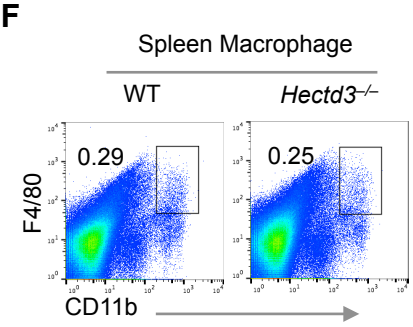

G

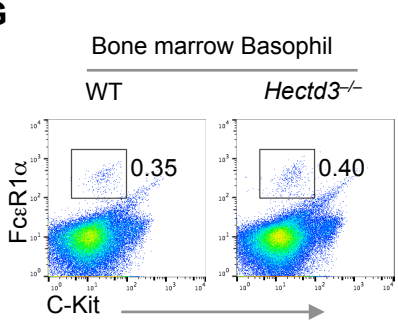

Supplemental Figure 1

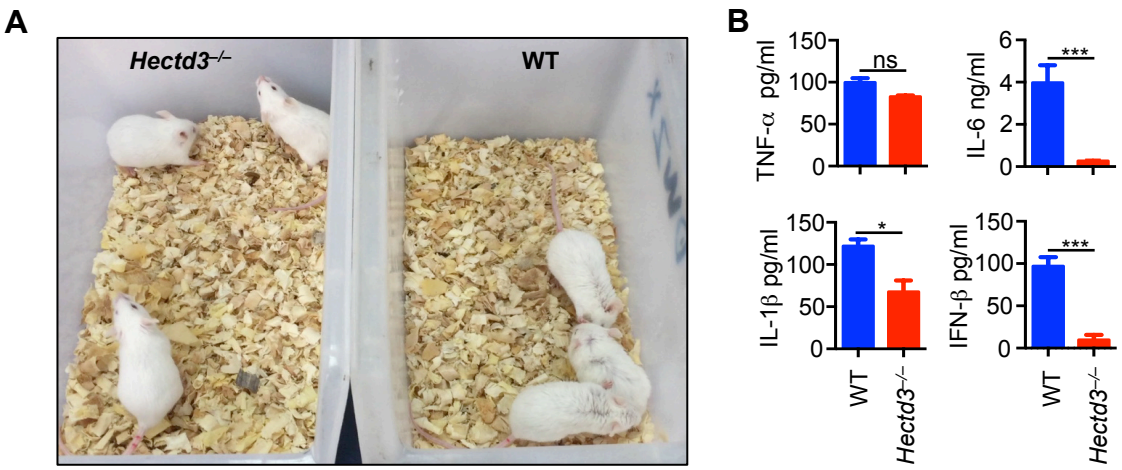

Supplemental Figure 2

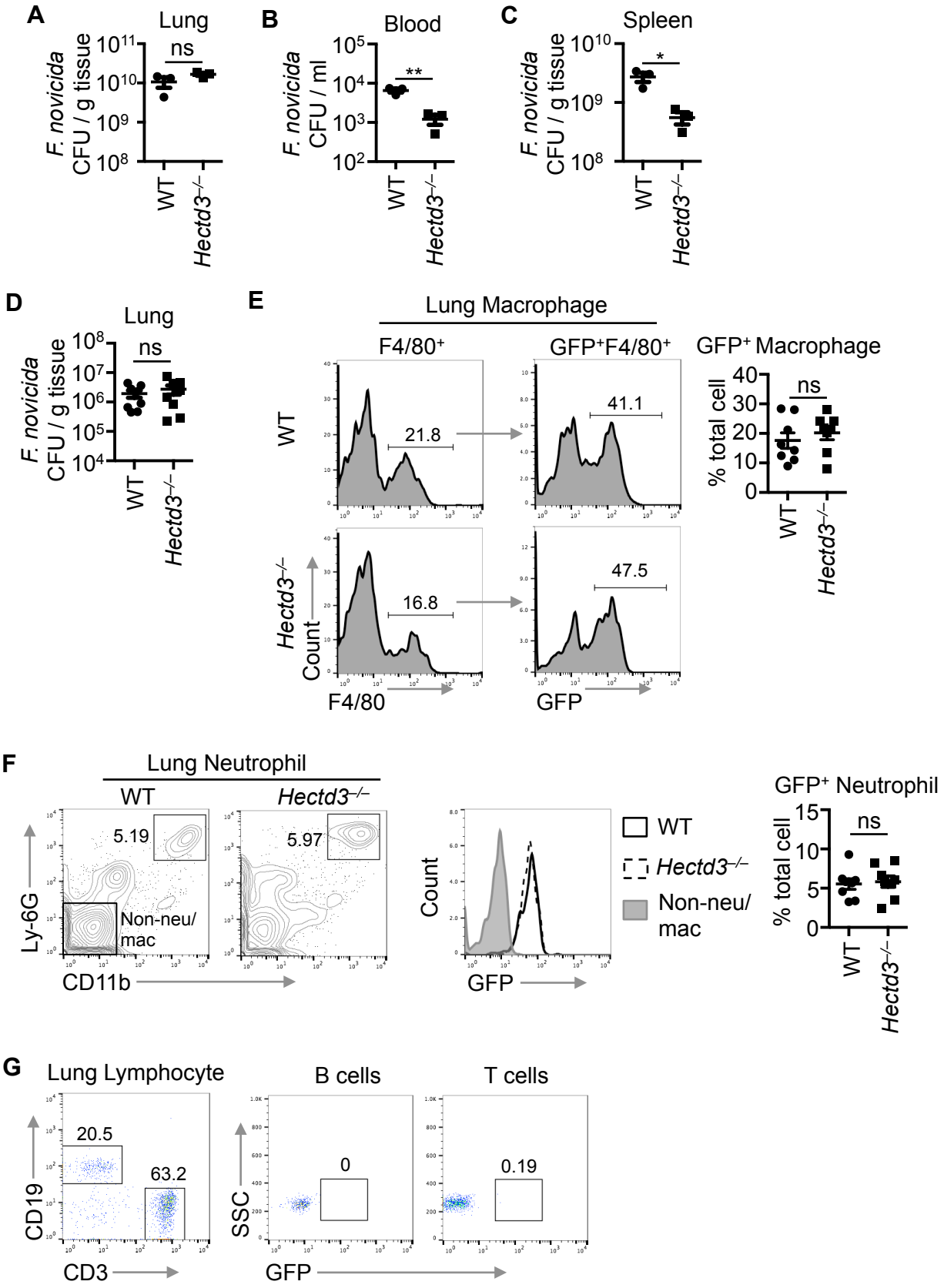

Supplemental Figure 3

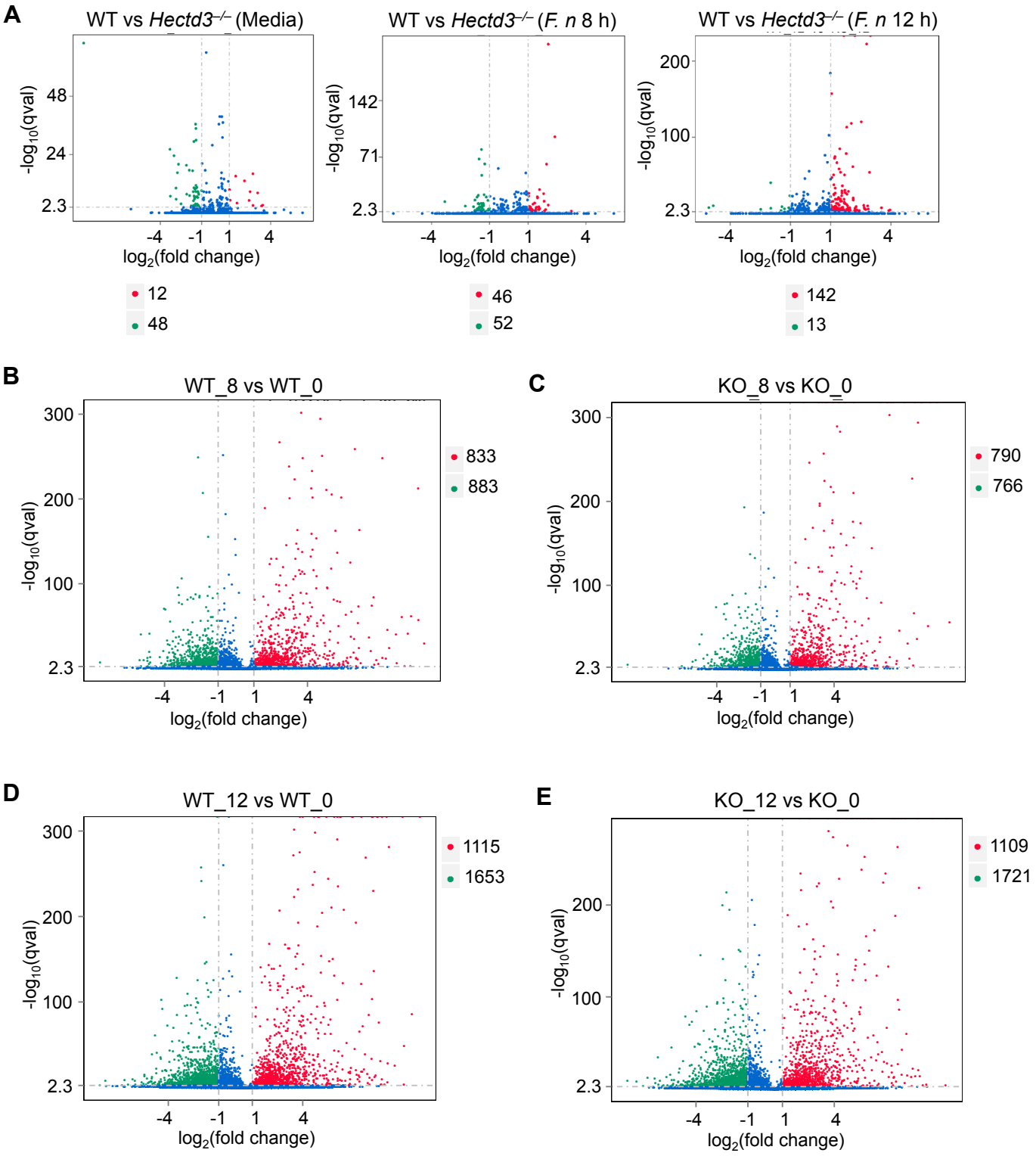

Supplemental Figure 4

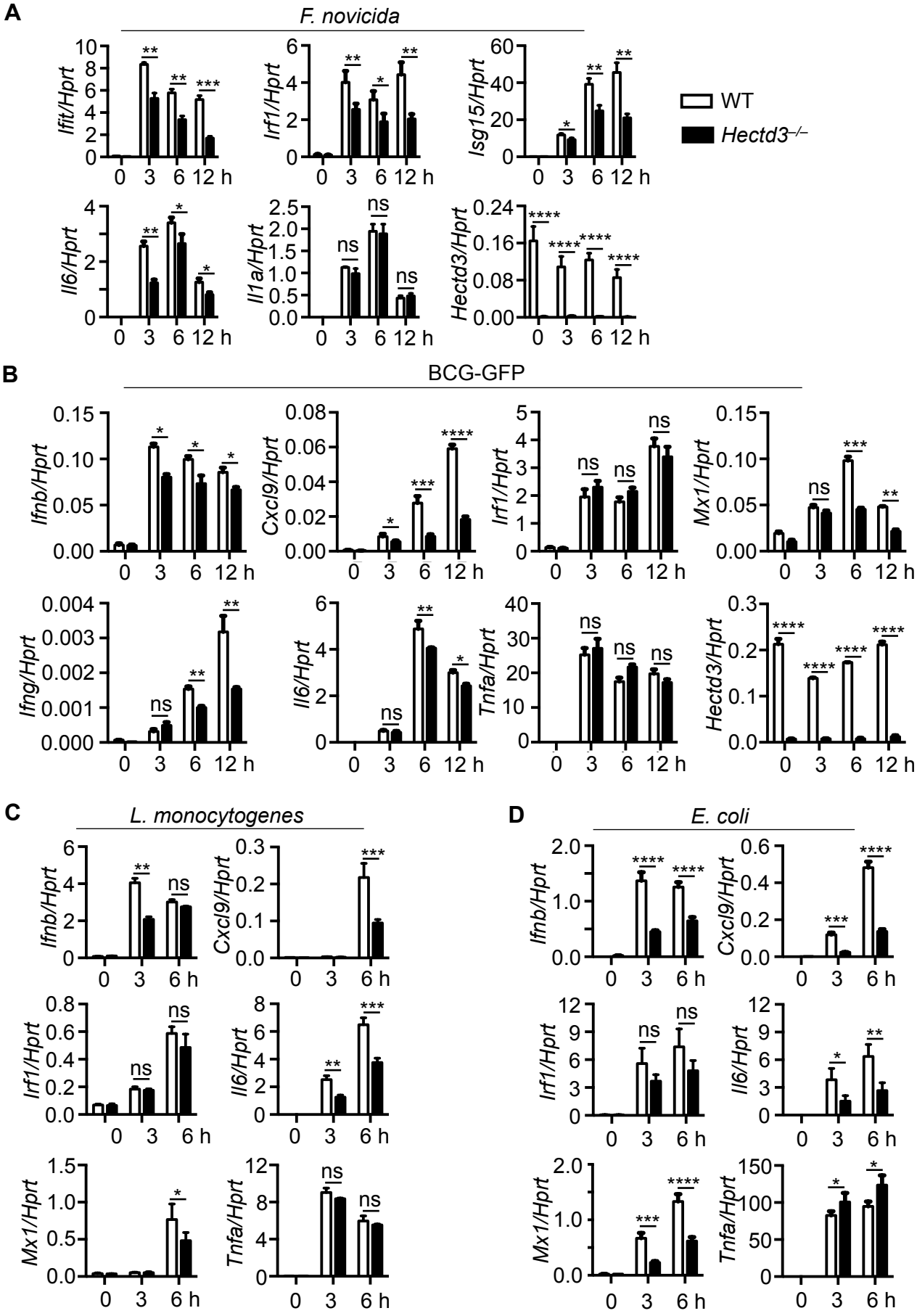

Supplemental Figure 5

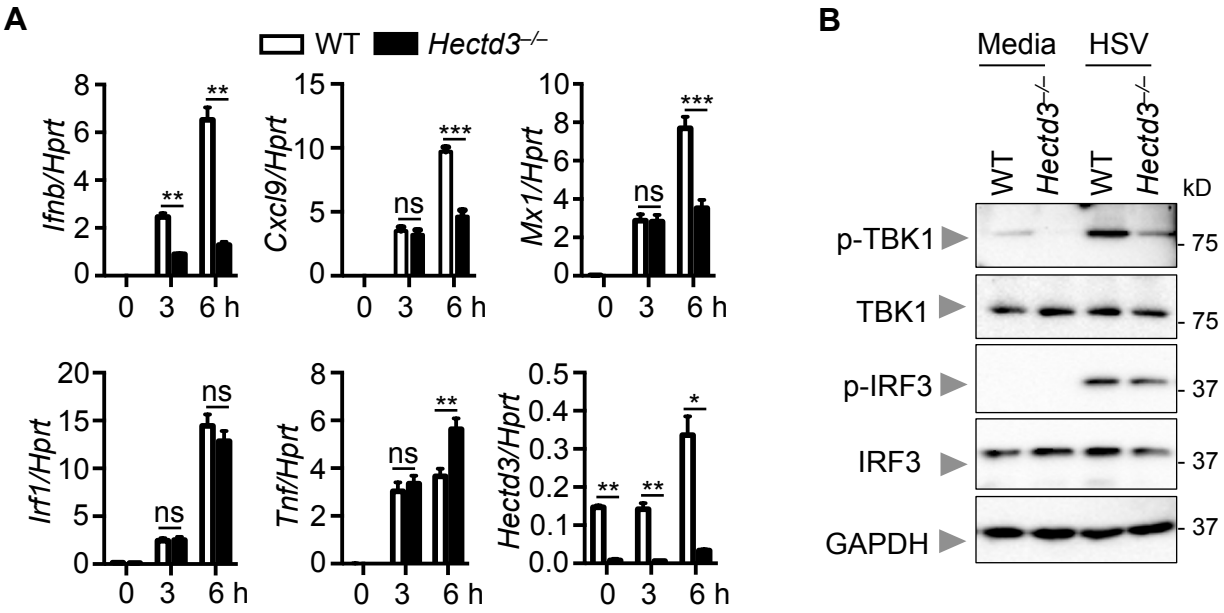

Supplemental Figure 6

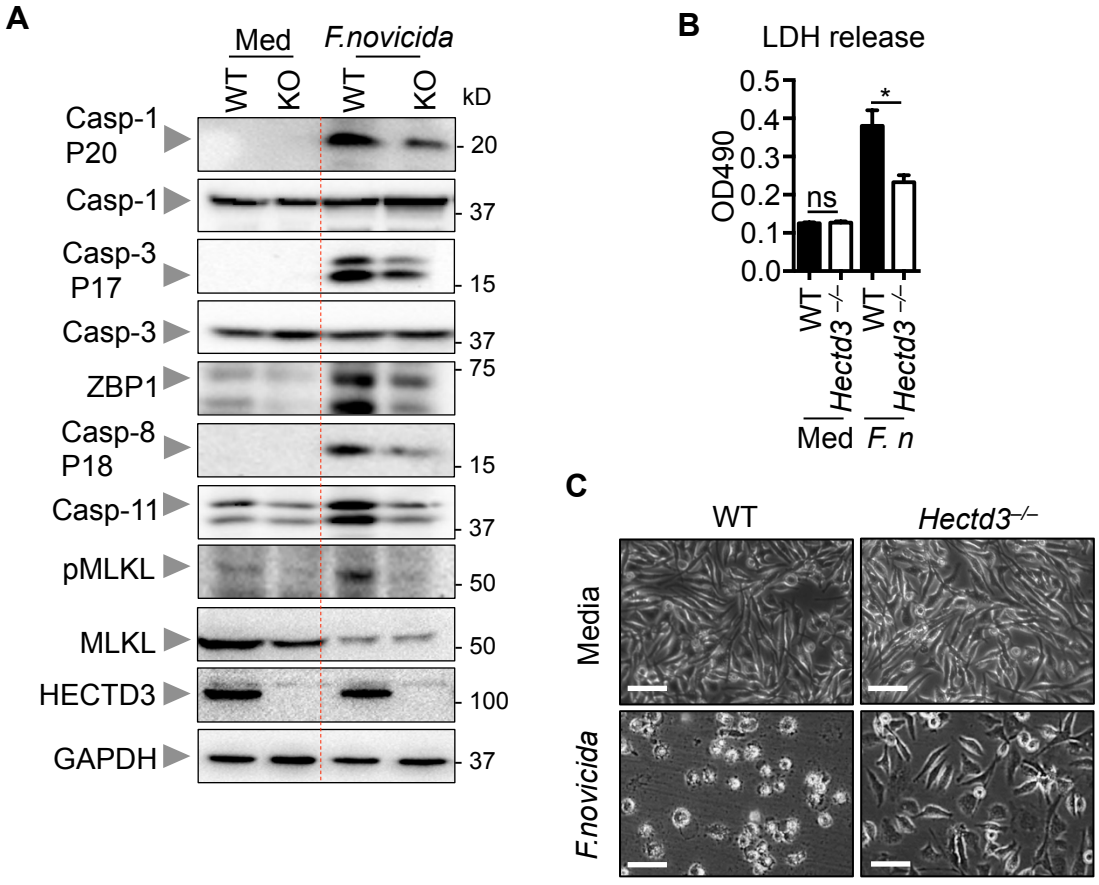

Supplemental Figure 7

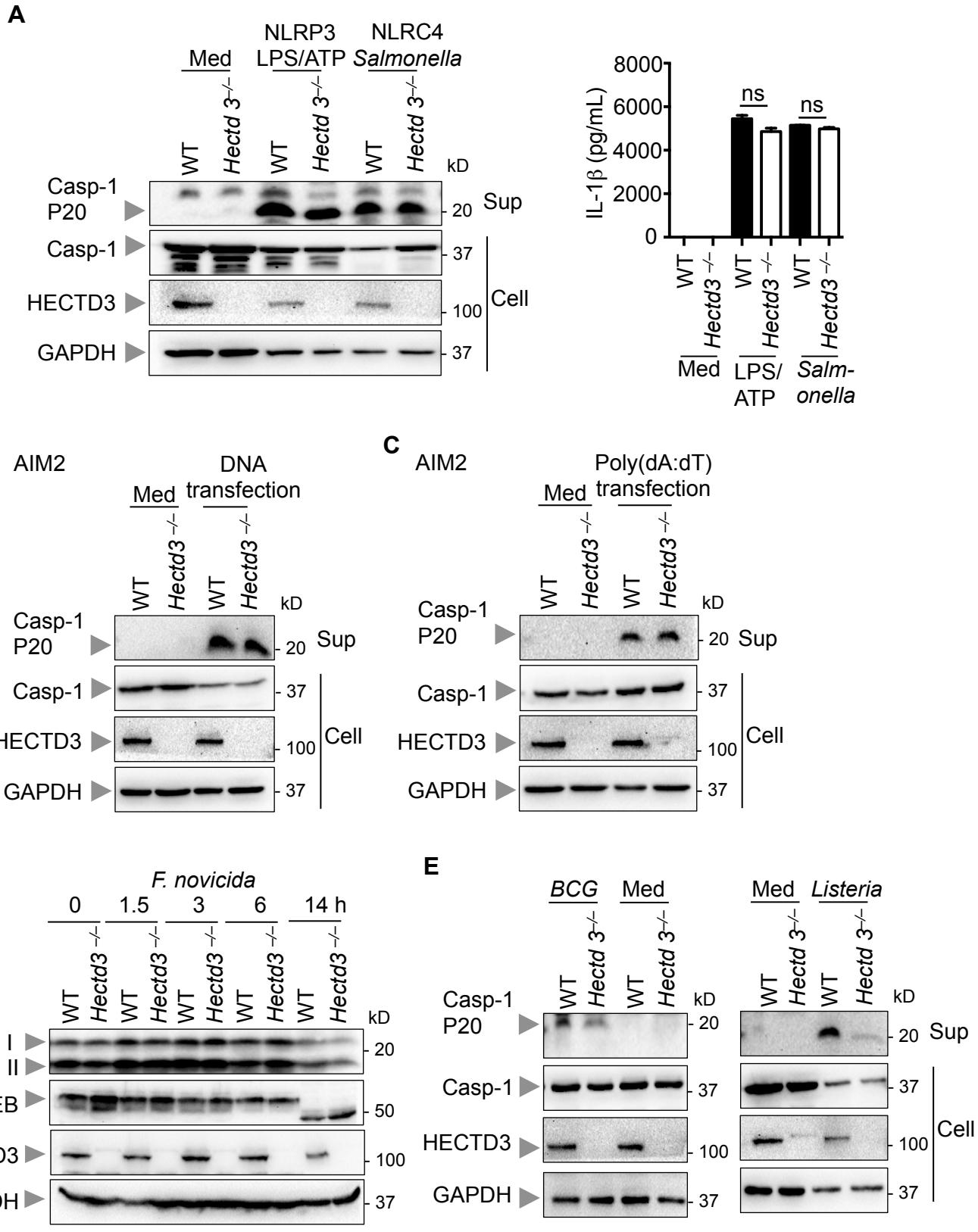

Supplemental Figure 8

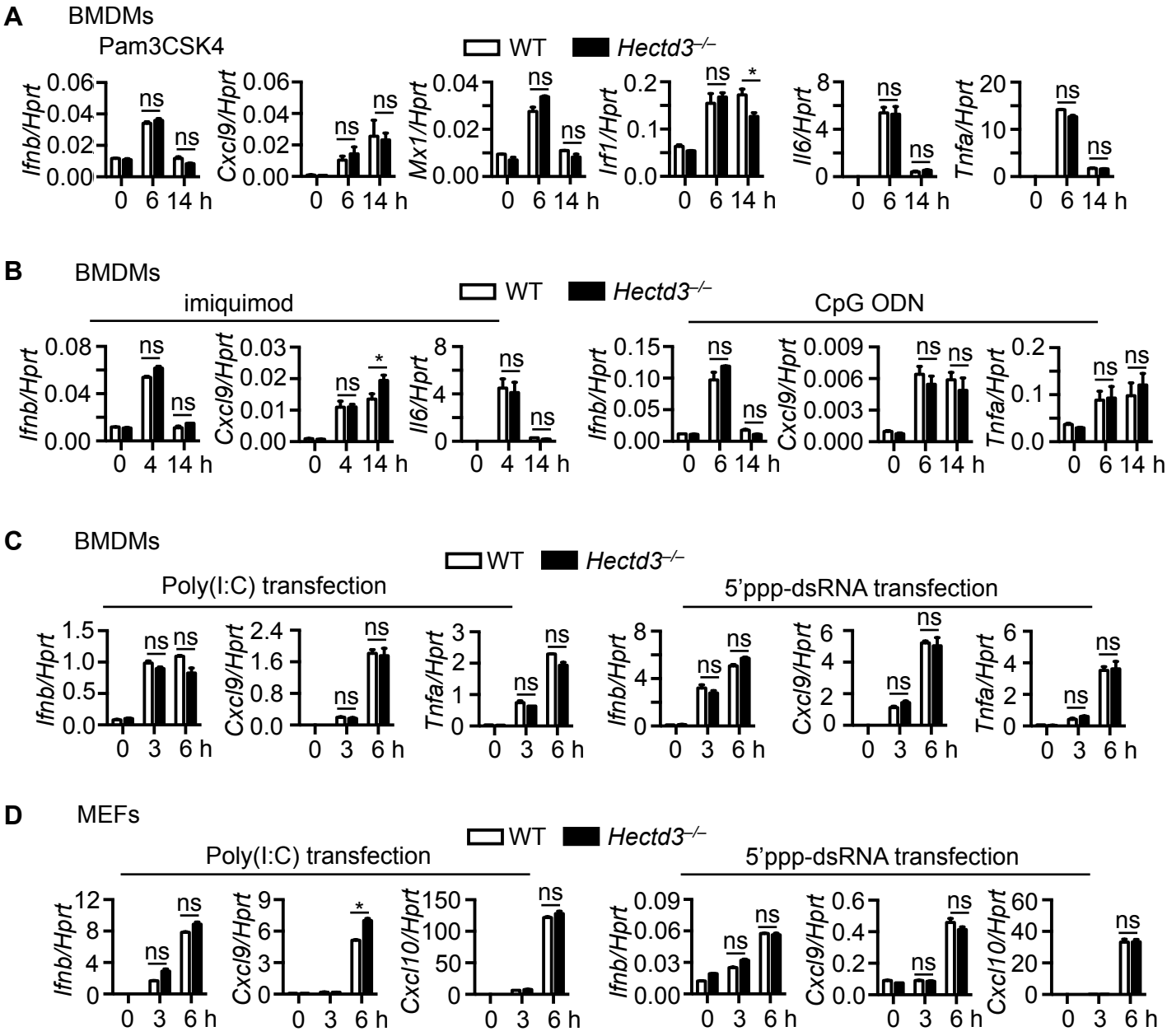

Supplemental Figure 9

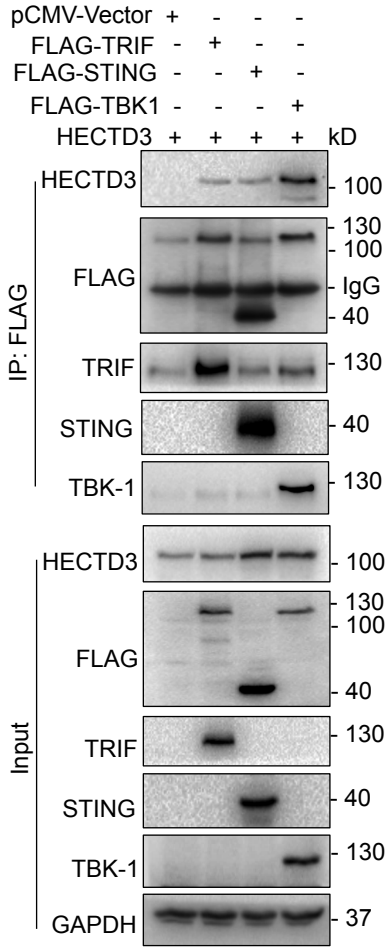

Supplemental Figure 10

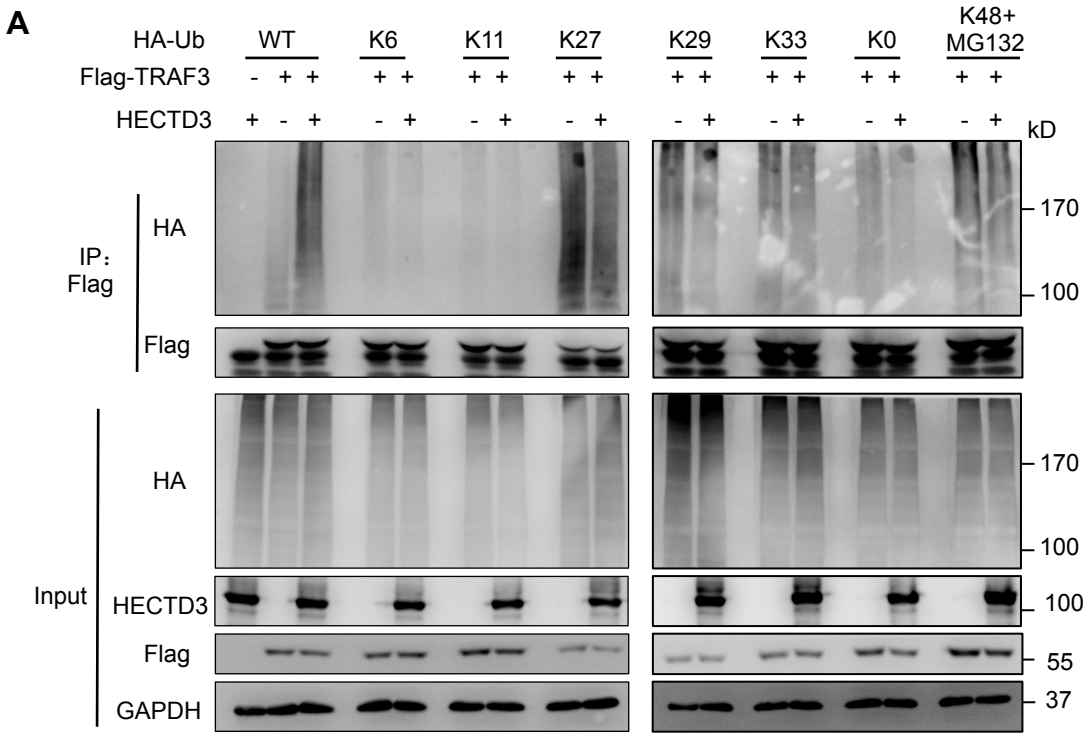

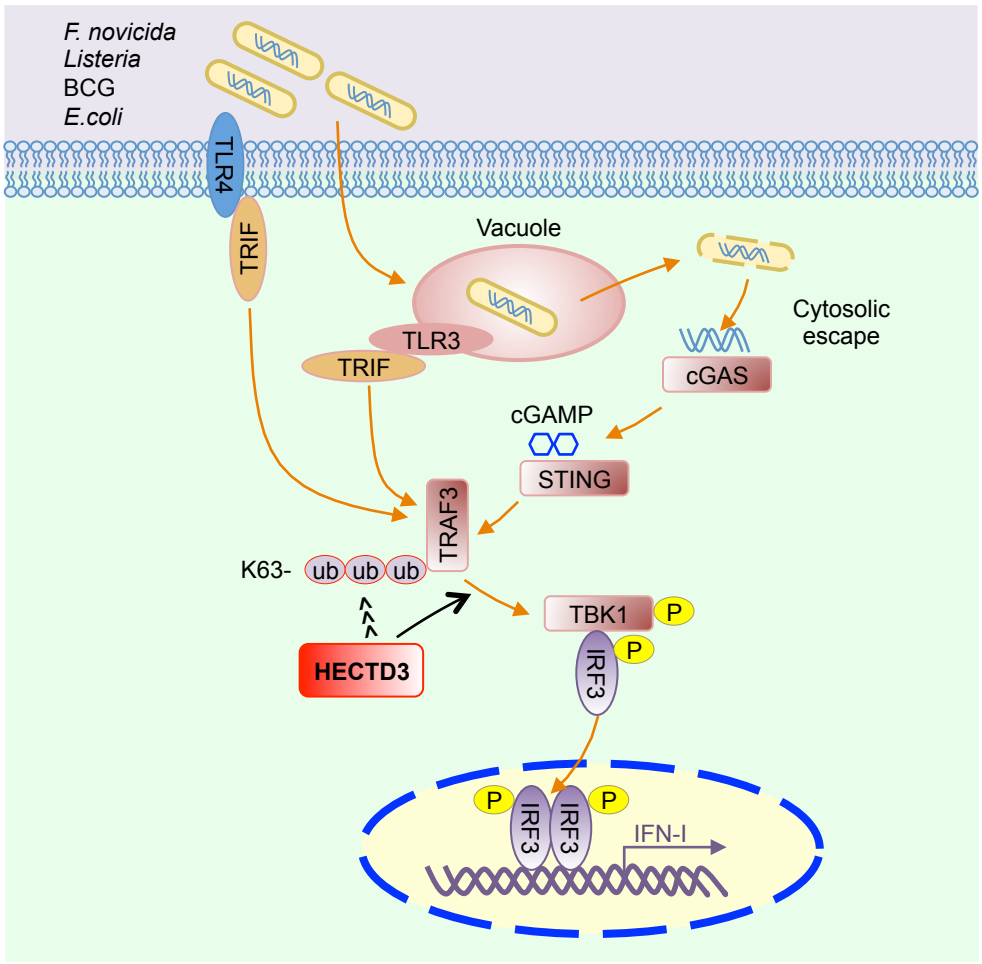

Supplemental Figure 11